



## Gold Nanoparticle-Based Electrochemical Sensor for the Detection of Toxic Metal Ions in Water

Seung Hye Choi, Jai-Pil Choi\*

Department of Chemistry, California State University – Fresno, 2555 East San Ramon Avenue, M/S SB70,  
Fresno, California 93740, United States of America  
Corresponding Author: Jai-Pil Choi

Received 01 September, 2017; Accepted 13 September, 2017 © The author(s) 2017. Published with open access at [www.questjournals.org](http://www.questjournals.org)

**ABSTRACT:** A simple, cost-effective, reusable electrochemical sensor (electronic tongue) that can simultaneously and accurately detect cadmium, mercury, lead, and arsenic ions in water was developed. Gold nanoparticles with approximately 1.6 nm core diameter were synthesized and their surfaces were functionalized with four different types of crown ethers that can selectively form complexes with  $Cd^{2+}$ ,  $Hg^{2+}$ ,  $Pb^{2+}$ , and  $As^{3+}$ . Thin films of these gold nanoparticles were casted on four interdigitated array (IDA) electrodes, individually responsible for the detection of specific metal ions. Then, four IDA electrodes were integrated to build an electronic tongue. Each IDA electrode of electronic tongue showed linear responses in conductance and junction potential with a specific metal ion, except for the  $As^{3+}$ -sensing IDA electrode. The detection limits were determined to 0.5 – 24.0 nM (0.1 – 2.7 ppb) for  $Hg^{2+}$ ,  $Pb^{2+}$ , and  $Cd^{2+}$ . Selectivity was studied by determining selectivity coefficients over six interfering ions. Both conductance and junction potential measurements showed similar selectivity.

**Keywords:** Conductance, Gold Nanoparticles, Heavy Metal, Junction Potential, and Sensor

### I. INTRODUCTION

Many metal ions are related to our lives in a variety of roles. Accurately monitoring the level (concentration) of metal ions is important to maintain a healthy life and safe environment. Some heavy metal ions ( $Fe^{2+}$ ,  $Zn^{2+}$ ,  $Cu^{2+}$ ,  $Co^{2+}$ ,  $Mn^{2+}$ , and  $Mo^{6+}$ ) are essential for human metabolism, but high concentration of these ions can lead to adverse health effects. [1, 2] In contrast, toxic heavy metal ions such as  $Hg^{2+}$ ,  $Cd^{2+}$ ,  $Pb^{2+}$ , and  $As^{3+}$ , can be dangerous threats; a small amount can cause irreversible damage to human health and the environment. [3–8] As shown in Table 1, the U.S. environmental protection agency (EPA) regulates the level of these ions, and local and/or state governments regularly monitor the quality of water, which includes the level of toxic metal ions. Thus, the accurate detection of such metal ions is an important topic in analytical chemistry, toxicology, and environmental science.

There are numerous analytical methods (e.g., atomic spectroscopy, inductively coupled plasma mass spectrometry, anodic stripping voltammetry, etc.), which can accurately and precisely measure a trace amount of metal ions. Moreover, considerable efforts have been devoted to the development of new methods that provide high sensitivity and selectivity; low power and sample consumption; ease of portability and use; fast and continuous on-site detection (or monitoring); low cost; reusability; and wide dynamic range. [9–11] To date, however, the detection method satisfying all of such merits has not been realized yet.

An electrochemical method furnished with nanomaterials is probably most promising to satisfy those requirements described above. Electrochemistry can provide high sensitivity, good selectivity, low cost, and ease of portability and use. [12] A glucose sensor that we can purchase for home use is a good exemplary device that takes the advantages of electrochemistry. Generally, nanomaterials have size- and surface-dependent properties [13], and employing nanomaterials for a sensing (or detecting) platform can further improve such merits as described above. Low sample consumption and miniaturization of a device are also possible, because of their much higher surface area to volume ratios than their bulk counter-parts [14].

**Table 1.** List of Toxic Metal Ions and Their Health Effects & Source. [8]

Metal Ion	MCLG <sup>a</sup> (ppm)	MCL <sup>b</sup> (ppm)	Health Effect	Source
Cd <sup>2+</sup>	0.000	0.010	Skin damage or problems with circulatory systems and increased risk of getting cancer	Erosion of natural deposits; runoff from orchards, runoff from glass and electronic production waste
Hg <sup>2+</sup>	0.005	0.005	Kidney damage	Corrosion of galvanized pipes; erosion of natural deposits; discharge from metal refineries; runoff from waste batteries and paints
Pb <sup>2+</sup>	0.000	0.015	Delays in physical or mental development; deficits in attention span and learning abilities; kidney problems; high blood pressure	Corrosion of household plumbing systems; erosion of natural deposits
As <sup>3+</sup>	0.002	0.002	Kidney damage	Erosion of natural deposits; discharge from refineries and factories; runoff from landfills and croplands

*a.* Maximum Contaminant Level Goal (MCLG) - The level of a contaminant in drinking water below which there is no known or expected risk to health. *b.* Maximum Contaminant Level (MCL) - The highest level of a contaminant that is allowed in drinking water.

Of nanomaterials, gold nanoparticles (Au NPs) are good candidate materials to make a versatile platform for chemical sensors, because (i) the functionalization toward selective and specific recognition of target analytes is possible on the surface of Au NPs; (ii) they display surface-dependent properties which can be utilized for the binding event with target analytes; (iii) the functionalized Au NPs may act as both target receptors and signal transducers on a sensor platform, allowing to simplify the sensor design; and (iv) they are relatively more stable from rusting than any other metal nanoparticles. [15, 16] Therefore, we chose Au NP as sensing materials to build sensor platforms. Using an electrochemical sensor made with Au NPs, we report here the detection of Cd<sup>2+</sup>, Pb<sup>2+</sup>, Hg<sup>2+</sup>, and As<sup>3+</sup> in water.

## II. EXPERIMENTAL SECTION

### 2.1. Chemicals

Tetrachloroauric acid trihydrate (HAuCl<sub>4</sub>·3H<sub>2</sub>O, > 99.99%), tetraoctylammonium bromide (TOA<sup>+</sup>Br<sup>-</sup>, 98%), *n*-hexanethiol (C<sub>6</sub>SH, 98%), sodium borohydride (NaBH<sub>4</sub>, ≥ 99%), tetrathia-12-crown-4 (CE1, 98%), hexathia-18-crown-6-tetraone (CE2, 98%), dibenzodiazia-15-crown-4 (CE3, 98%), 12-crown-4 (CE4, 98%), and 1,11-dibromoundecane (≥ 98%) were obtained from Sigma-Aldrich and used as received. Toluene, acetonitrile, methylene chloride, and methanol were purchased from Fisher Scientific (all Optima grade solvents). Deionized (DI) water (> 18 MΩ) produced from a Barnstead Fistream II purification system was used in all syntheses and preparations.

### 2.2. Synthesis of Gold Nanoparticles

Au NPs were synthesized with the known methods [17, 18]. 3.1 g of HAuCl<sub>4</sub>·3H<sub>2</sub>O were dissolved in 100-mL deionized (DI) water. This solution was mixed with 200-mL toluene solution containing 5.6 g TOA<sup>+</sup>Br<sup>-</sup>, followed by stirring vigorously for 30 minutes. The aqueous phase was removed but the toluene phase was collected for the next step, using a separatory funnel. 3.36 mL of C<sub>6</sub>SH were added to the collected toluene solution, where AuCl<sub>4</sub><sup>-</sup> ions were contained. This solution was stirred until its reddish brown color changed to the clear transparent, indicating that polymeric hexanethiolated Au(I) compounds were produced. After that, the solution was placed in an ice bath to maintain its temperature to 0 °C. 50 mL of the aqueous solution, in which 3.8g NaBH<sub>4</sub> were dissolved, quickly poured into the cooled solution to reduce polymeric hexanethiolated Au(I) compounds to Au NPs. This two-phase solution (toluene and aqueous NaBH<sub>4</sub>) were vigorously stirred for 2 hours. The toluene phase, where Au NPs were formed, was collected using a separatory funnel. The solvent, toluene, was removed at a reduced pressure, and formed Au NPs were extracted with ethanol. The obtained Au NPs were further purified with acetonitrile and ethanol, until Au<sub>140</sub>(SC6)<sub>53</sub> nanoparticles were obtained. The formed Au<sub>140</sub>(SC6)<sub>53</sub> were confirmed by comparing data obtained electrochemistry and UV-Vis absorption spectroscopy with the literature data [18].

### 2.3. Ligand Exchange Reactions and Functionalization

The synthesized Au NPs, Au<sub>140</sub>(SC6)<sub>53</sub>, were functionalized with four different types of crown ethers: CE1, CE2, CE3, and CE4 for the detection of Cd<sup>2+</sup>, Hg<sup>2+</sup>, Pb<sup>2+</sup>, and As<sup>3+</sup> (Fig. 1). The linker molecule, 1-bromoundecane- $\omega$ -thiol, was attached on a carbon atom of the crown ether ring by a substitution reaction [19]. Functionalization of Au NPs was achieved by ligand exchange reactions [20] with thiolated crown ethers. For

this, 30.0 mg of  $\text{Au}_{140}(\text{SC6})_{53}$  were dissolved in 10.0-mL dichloromethane ( $\text{CH}_2\text{Cl}_2$ ), followed by addition of a 3-fold excess amount (with respect to the moles of SC6 on a nanoparticle) of a target crown ethers (CE1 – 4). For example, 0.103 g of CE1 were added to the solution of 30.8 mg  $\text{Au}_{140}(\text{SC6})_{53}$ . After this reaction mixture was stirred for 24 hours, the solvent,  $\text{CH}_2\text{Cl}_2$ , was removed at a reduced pressure with a rotary evaporator. The obtained solid reaction product was washed with heptane until the extra CE1 and the out-coming SC6 thiols were removed. With this procedure, four different types of functionalized Au NPs were prepared:  $\text{Au}_{140}(\text{CE1})$ ,  $\text{Au}_{140}(\text{CE2})$ ,  $\text{Au}_{140}(\text{CE3})$ , and  $\text{Au}_{140}(\text{CE4})$ .

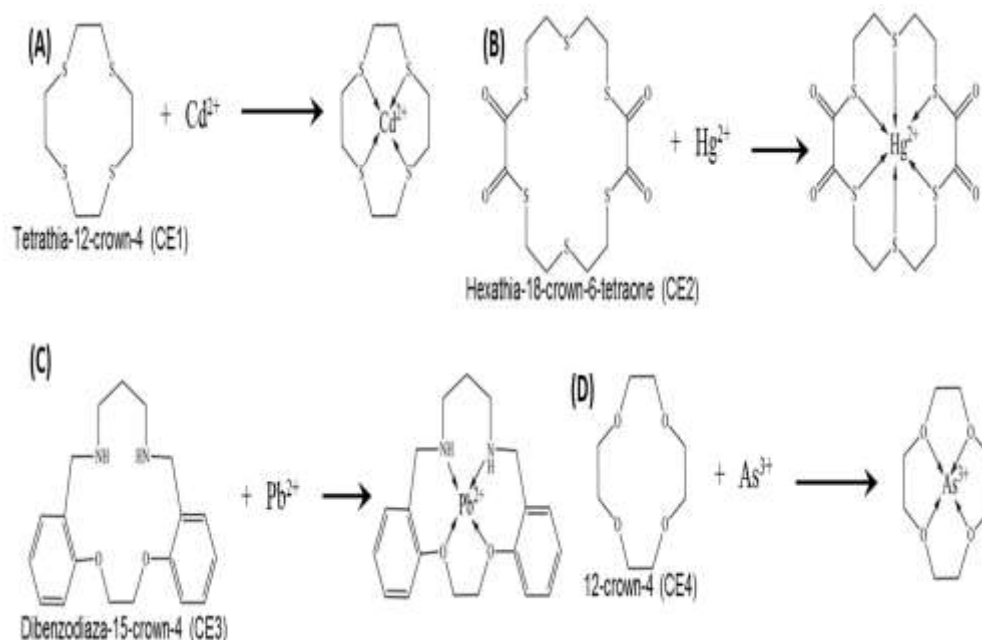


**Figure 1.** Molecular structures of crown ethers and their reaction schemes for complexation of (A)  $\text{Cd}^{2+}$ , (B)  $\text{Hg}^{2+}$ , (C)  $\text{Pb}^{2+}$ , and (D)  $\text{As}^{3+}$  with crown ethers.

#### 2.4. Preparation of Individual Sensor Platforms

The individual sensor platforms were constructed with interdigitated array (IDA) electrodes, on which thin films of functionalized Au NPs were drop-casted. The IDA electrodes obtained from Abtech Scientific, Inc. (Richmond, VA) contain 25 pairs of finger electrodes (3 mm finger length, 20  $\mu\text{m}$  finger width, 180 nm finger height, and 20  $\mu\text{m}$  separation gap).

#### 2.5. Electrochemical Measurements

A CHI660C potentiostat (CH Instruments, Austin, TX) or four-channel potentiostat (Gamry Instruments, Warminster, PA) was used for electrochemical measurements. Cyclic voltammetry was employed to obtain the conductance data, and so was chronopotentiometry to obtain the liquid junction potential data.

### III. RESULTS

#### 3.1. Selection of Crown Ethers for functionalization of Au NPs

It is well known that the crown ethers (CE1 – 4) shown in Figure 2 can selectively form complexes with  $\text{Cd}^{2+}$ ,  $\text{Hg}^{2+}$ ,  $\text{Cd}^{2+}$ , and  $\text{As}^{3+}$ . Therefore, the four different types of crown ethers were chosen to functionalize the surface of Au NPs (Fig. 1). As described in Experimental Section, the functionalization of  $\text{Au}_{140}(\text{SC6})_{53}$  was achieved by ligand exchange reactions [20]. The functionalized Au NPs,  $\text{Au}_{140}(\text{CE1})$ ,  $\text{Au}_{140}(\text{CE2})$ ,  $\text{Au}_{140}(\text{CE3})$ , and  $\text{Au}_{140}(\text{CE4})$  are shown in Fig. 2. The number of crown ether ligands exchanged in each reaction (Figure 3) was not analyzed. However, it was possible to make a rough estimation, ~65 – 70% exchange rate, using the reference data [20]. Note that Fig. 2 shows only schematic illustrations; not all surface-protecting ligands (SC6) nor functional ligands (CE1 – 4).

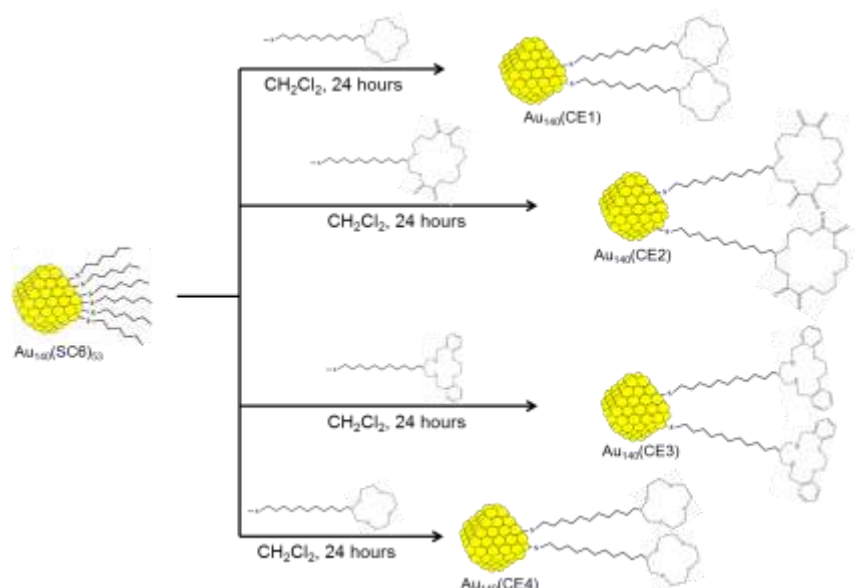


**Figure 2.** Illustration of ligand exchange reactions to functionalize  $\text{Au}_{140}(\text{SC6})_{53}$  with CE 1 – 5. The exchange rate was about 65 – 70%. Note that the figure shows only schematic illustration; not all surface-protecting ligands (SC6) nor functional ligands (CE1 – 4)

### 3.2. Preparation of Electrochemical Sensor Platforms

The sensing platforms of an electrochemical sensor array were prepared with four IDA electrodes and functionalized Au-NP films on them. Each IDA electrode had a differently functionalized Au-NP film ( $\sim 1 \mu\text{m}$  thick) and was responsible for the detection of different toxic metal ions as shown in Fig. 3A. For example, the IDA electrode with an  $\text{Au}_{140}(\text{CE1})$  film were used to detect  $\text{Cd}^{2+}$ . Four IDA electrodes were integrated into a sock adaptor to construct the electrochemical sensor array (Fig. 3B). The IDA electrodes of the electrochemical sensor array were independently connected to a four-channel potentiostat for signal-processing. The size of each IDA electrode is 1.0 (length)  $\times$  0.5 (width)  $\times$  0.05 (thickness) cm, and the overall size of the electronic tongue is 3.0 (length)  $\times$  4.0 (width)  $\times$  2.5 (height) cm.

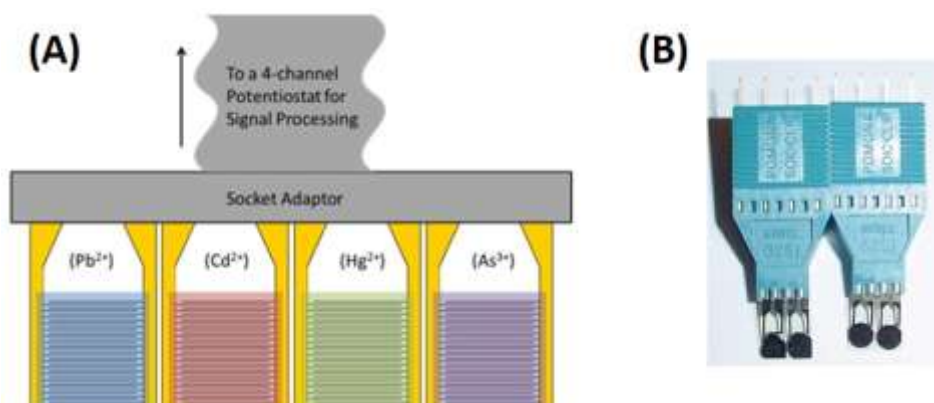


**Figure 3.** (A) Illustration of the electrochemical sensor array design and (b) the actual electrochemical sensor array prepared for this work.

### 3.3. Calibration of the Electrochemical Sensor Array

Both conductance and liquid junction potential were measured to calibrate the electronic tongue. 1.0 ppb – 100 ppm standard solution of  $\text{Cd}^{2+}$ ,  $\text{Hg}^{2+}$ ,  $\text{Pb}^{2+}$ , and  $\text{As}^{3+}$  were used. As shown in Figure 5(a), conductance of Au-NP films on electronic tongue was determined from the slope of a cyclic voltammograms. The current response ( $I$ ) was linear with respect to voltage ( $V$ ) applied. By Ohm's law,  $I = (1/R) \cdot V$  [21], the slope is conductance ( $1/R$ ). The measured conductance was normalized by dividing it with the conductance measured in the absence of toxic metal ions. Normalized conductance was linearly increased as the concentrations of  $\text{Cd}^{2+}$ ,  $\text{Hg}^{2+}$ , and  $\text{Pb}^{2+}$  increased, but the conductance measured from  $\text{As}^{3+}$  standard solutions was independent of the concentration of  $\text{As}^{3+}$  (Figs. 4B and 4C). Note that the scale of normalized conductance

in Fig. 4C relatively smaller than that in Fig. 4B. Also the normalized conductance at and after 0.1 ppm  $\text{As}^{3+}$  was completely independent of its concentration.

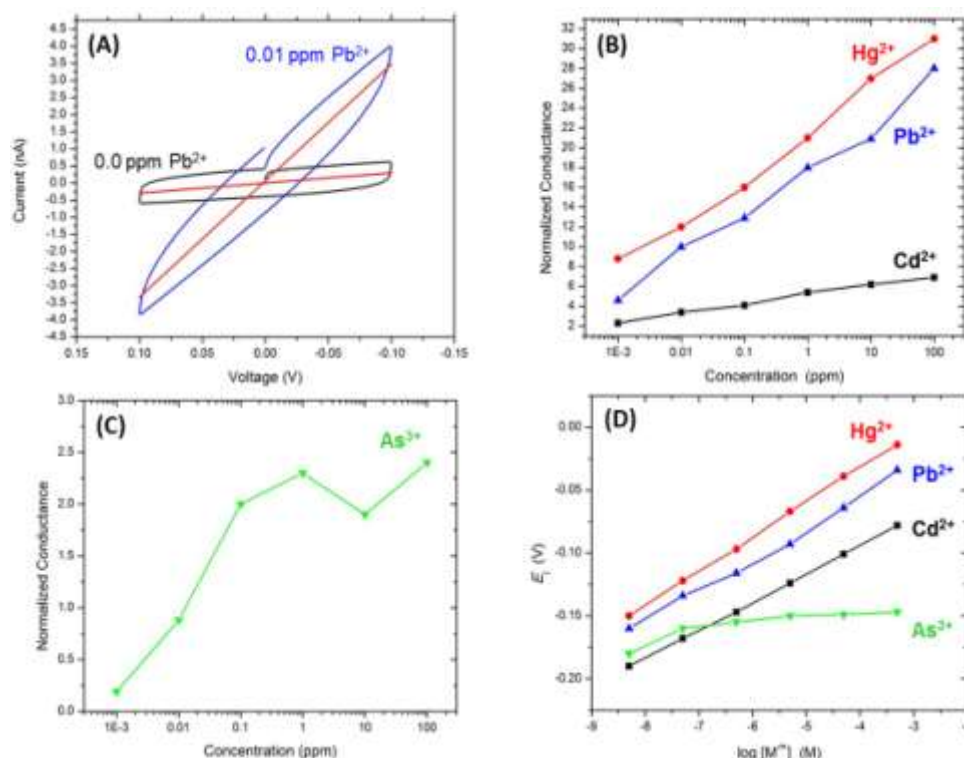


**Figure 4.** (A) Cyclic voltammograms of 0.000 and 0.100 ppm  $\text{Pb}^{2+}$  measured from an  $\text{Au}_{140}(\text{CE}3)$  film. (B) Calibration plots of  $\text{Hg}^{2+}$ ,  $\text{Pb}^{2+}$ , and  $\text{Cd}^{2+}$  made with conductance. (C) Calibration plot of  $\text{As}^{3+}$  made with conductance. (D) Calibration plots of  $\text{Cd}^{2+}$ ,  $\text{Hg}^{2+}$ ,  $\text{Cd}^{2+}$ , and  $\text{As}^{3+}$  made with liquid junction potential ( $E_j$ ).

When an Au-NP film contacts with a sample solution, liquid junction potential ( $E_j$ ) is developed at the interface between the film surface and liquid. By the modified Nernst equation [21] below, the measured  $E_j$  is linearly proportional to the logarithmic concentration of toxic metal ions:

$$E_j = \left( \frac{RT}{nF} \right) \ln[M^{n+}] + C = \frac{0.0592}{n} \log[M^{n+}] + C \quad (1)$$

where  $R$  is the gas constant ( $8.314 \text{ J} \cdot \text{mol}^{-1} \cdot \text{K}^{-1}$ ),  $T$  is temperature in Kelvin,  $n$  is the number of electrons transferred,  $F$  is Faraday's constant ( $96,485 \text{ C/mol}$ ),  $[M^{n+}]$  is the concentration of metal ions, and  $C$  is an arbitrary constant. For  $\text{Cd}^{2+}$ ,  $\text{Hg}^{2+}$ , and  $\text{Pb}^{2+}$  ions, the measured  $E_j$  became more positive as their concentrations increased (Fig. 4D). However,  $E_j$  measured in the presence of  $\text{As}^{3+}$  was independent of its concentration (Fig. 4D).

### 3.4. Detection Limits and Selectivity

The detection limits (DL) were statistically determined from a calibration plot [22]:  $\text{DL} = 3 \cdot \text{SD}/\text{slope}$ , where SD denotes standard deviation of linear regression slope on the calibration. The determined DL data were summarized in Table 2. Because both conductance and  $E_j$  of  $\text{Au}_{140}(\text{CE}4)$  films were independent of the concentration of  $\text{As}^{3+}$ , the DL of  $\text{As}^{3+}$  could not be determined.

**Table 2.** Detection Limits of Toxic Metal Ions

Metal Ion	Detection Limit Determined from Conductance	Detection Limit Determined from Liquid Junction Potential
$\text{Cd}^{2+}$	2.7 ppb (24.0 nM)	0.1 ppb (0.63 nM)
$\text{Hg}^{2+}$	1.2 ppb (6.0 nM)	0.09 ppb (0.47 nM)
$\text{Pb}^{2+}$	1.8 ppb (8.7 nM)	0.1 ppb (0.55 nM)
$\text{As}^{3+}$	- <sup>a</sup>	- <sup>a</sup>

a. They could not be determined because both conductance and  $E_j$  were independent of the concentration of  $\text{As}^{3+}$ .

The selectivity coefficients ( $K_{A,X}$ ) were determined by measuring the response from interfering ions, such as  $K^+$ ,  $Mg^{2+}$ ,  $Ca^{2+}$ , and the other three metal ions (for example,  $Hg^{2+}$ ,  $Pb^{2+}$ , and  $As^{3+}$  are interfering ions at the  $Cd^{2+}$ -detecting IDA electrode of electronic tongue). The measured interference responses were compared with the response from the target analyte ions in order to calculate  $K_{A,X}$  [23]:

$$K_{A,X} = \frac{\text{Response of Interfering Ion (X)}}{\text{Response of Analyte Ion (A)}} \quad (2)$$

where response is either normalized conductance or  $E_j$ . The calculated  $K_{A,X}$  data are summarized in Table 3.

**Table 3.** Selectivity Coefficients of  $Cd^{2+}$ -,  $Hg^{2+}$ -, and  $Pb^{2+}$ -Detecting Electrodes Integrated on the Electrochemical Sensor Array

Interfering Ion	$Cd^{2+}$ -Detecting IDA		$Hg^{2+}$ -Detecting IDA		$Pb^{2+}$ -Detecting IDA	
	$K_{Cd,X}$ ( $\times 10^{-3}$ ) <sup>a</sup>	$K_{Cd,X}$ ( $\times 10^{-3}$ ) <sup>b</sup>	$K_{Hg,X}$ ( $\times 10^{-3}$ ) <sup>a</sup>	$K_{Hg,X}$ ( $\times 10^{-3}$ ) <sup>b</sup>	$K_{Pb,X}$ ( $\times 10^{-3}$ ) <sup>a</sup>	$K_{Pb,X}$ ( $\times 10^{-3}$ ) <sup>b</sup>
$K^+$	0.5	0.3	4.0	2.0	1.3	1.0
$Mg^{2+}$	4.2	1.3	3.6	3.8	5.9	0.4
$Ca^{2+}$	5.9	0.8	6.6	6.2	5.2	3.1
$Cd^{2+}$	-	-	4.1	0.3	3.0	4.7
$Hg^{2+}$	0.5	0.5	-	-	3.8	2.5
$Pb^{2+}$	4.1	0.2	5.2	1.0	-	-
$As^{3+}$	$\sim 0$					

a. Determined by conductance. b. Determined by liquid junction potential.

**Table 4.** Cavity Size of Crown Ethers Similar to CE1 – 4 and Ionic Diameters of Toxic Metal Ions

Crown Ether	Cavity Size (nm) <sup>a</sup>	Similar Crown Ether Used in This Work	Detectable Ion (Ion Size) <sup>b</sup>
12-crown-4	$\sim 0.12$	CE1 and CE4	$As^{3+}$ (0.14 nm)
14-crown-4	0.12 – 0.15	CE3	$Cd^{2+}$ (0.22 nm)
15-crown-5	0.17 – 0.22	CE3	$Hg^{2+}$ (0.23 nm)
18-crown-6	0.26 – 0.32	CE2	$Pb^{2+}$ (0.26 nm)

a. Obtained from Ref. [24]. b. Obtained from Ref. [25].

## IV. DISCUSSION

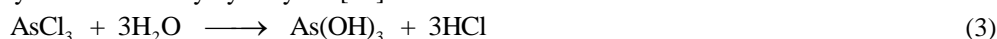
### 4.1. Selection of Crown Ethers for Functionalization of Au NPs

The selected crown ethers (CE1 – 4) can undergo selective complexation reactions with specific metal ions [26–29]. This selective complexation reaction is mainly governed by the nature of binding atoms (*e.g.*, O or S) on crown ether and the cavity (ring) size, although there are many other factors that affect it. When the cavity (ring) size of crown ethers is well matched with the size of metal ions, a more stable complex will be formed. Unfortunately, no cavity diameter data are available for CE1 – 4, but a rough estimation can be made with the cavity size of similar crown ethers as shown in Table 4.

### 4.2. Calibration, Detection Limits, Selectivity of the Electrochemical Sensor Array

When metal ions are complexed on functionalized Au-NP films casted on IDA electrodes (electronic tongue), conductance and  $E_j$  of films can be changed. In fact, conductance was enhanced, because the complexed metal ions serve as charge carriers. In the absence of metal ions, functionalized Au-NP films showed minimal conductance, while conductance became more enhanced with more metal ions complexed on a film. Similar trend was observed in  $E_j$  measurements.  $E_j$  is electrical potential developed at the interface when dissimilar phases make contact with each other. Therefore, a functionalized Au-NP film contacted with the solution of more concentrated metal ions results in higher  $E_j$ .

Comparing two calibrations obtained from conductance and  $E_j$  measurements (Figs. 4B and 4D), calibration by  $E_j$  seems to show better linear fits and sensitivities (higher slope of calibration plots) over all metal ions except for  $As^{3+}$  than that by conductance. Detection of  $As^{3+}$  was not successful with both conductance and  $E_j$ , due to the hydrolysis reaction of  $As^{3+}$ . When arsenic salts (*e.g.*,  $AsCl_3$ ) are dissolved in water, they are immediately hydrolyzed [30] as follows:



Once arsenous acid ( $\text{As}(\text{OH})_3$ ) is produced by hydrolysis (reaction 3), it deprotonates forming  $\text{AsO}_3^{3-}$  (reaction 4). The negatively charged oxygen atoms on  $\text{AsO}_3^{3-}$  prohibit the complexation reaction with functional crown ethers on Au NPs. Therefore, very weak or no response resulted.

Detection limits (0.1 – 3.0 ppb) of  $\text{Cd}^{2+}$ ,  $\text{Hg}^{2+}$ , and  $\text{Pb}^{2+}$  obtained in this project were much lower than the EPA-controlled levels (5 – 15 ppb). Because Au NPs has higher surface area-to-volume ratios than bulk materials, such low detection limits could be obtained. Moreover, the electrochemical sensor array developed in this work consumes an extremely low amount of sample (~ tens  $\mu\text{L}$ ) and power (voltage  $\times$  current). As shown in Fig. 4A, conductance can be successfully measured with  $\pm 0.1\text{V}$  bias along with ~ nA current range. Therefore, the maximum power consumed per measurements would be a few nW (1 nW =  $10^{-9}$  W), implying the developed electronic tongue can be operated with an AAA-size 1.5 V battery. The developed electronic tongue also shows excellent selectivity (Table 3): in most cases, the analyte signals are about 1000-fold higher than interference signal.

## V. CONCLUSION

The electrochemical sensor array was developed to detect toxic metal ions, using four different types of gold nanoparticles:  $\text{Au}_{140}(\text{CE}1)$ ,  $\text{Au}_{140}(\text{CE}2)$ ,  $\text{Au}_{140}(\text{CE}3)$ , and  $\text{Au}_{140}(\text{CE}4)$ . The developed electronic tongue shows good linear responses for the quantitative analysis of  $\text{Cd}^{2+}$ ,  $\text{Hg}^{2+}$ , and  $\text{Pb}^{2+}$ , but it does not for  $\text{As}^{3+}$  because of its hydrolysis reaction. It also shows excellent selectivity over  $\text{K}^+$ ,  $\text{Mg}^{2+}$ ,  $\text{Ca}^{2+}$ ,  $\text{Cd}^{2+}$ ,  $\text{Hg}^{2+}$ ,  $\text{Pb}^{2+}$ , and  $\text{As}^{3+}$ . The developed electronic tongue consumes low power, uses an extremely small volume of sample for analysis, and can be further miniaturized. Finally, the developed electronic tongue may be used to evaluate the water quality in terms of heavy metal ion contamination in accordance with the EPA regulation.

## ACKNOWLEDGEMENTS

It is gratefully acknowledged that this research was supported in part by grants from Research Corporation (CCSA10523), CSU Program for Education & Research in Biotechnology, Faculty-Sponsored Student Research Award.

## REFERENCES

- [1]. K. Jomova, S. Baros, and M. Valko, Redox Active Metal-Induced Oxidative Stress in Biological Systems, *Transition Metal Chemistry*, 37, 2012, 127-134.
- [2]. D. Caussy, M. Gochfeld, E. Gurzau, C. Neagu, and H. Ruedel, Lessons from Case Studies of Metals: Investigating Exposure, Bioavailability, and Risk, *Ecotoxicology and Environmental Safety*, 56, 2003, 45-51.
- [3]. S. Aldred and R.H. Waring, Mercury, in R.H. Waring, G.B. Steventon, and S.C. Mitchell (Eds.), *Molecules of Death*, 2nd ed. (London, UK: Imperial College Press, (2007) 167-185.
- [4]. P. Martin and P. Pognonec, ERK and Cell Death: Cadmium Toxicity, Sustained ERK Activation and Cell Death. *FEBS Journal*, 277, 2010, 39-46.
- [5]. M.A. Riva, A. Lafranconi, M.I. D'orso, and G. Cesana, Lead Poisoning: Historical Aspects of a Paradigmatic Occupational and Environmental Disease, *Safety and Health Work*, 3, 2012, 11-16.
- [6]. D.B. Ramsden and T. Pawade, Lead: An Old and Modern Poison, in R.H. Waring, G.B. Steventon, and S.C. Mitchell (Eds.), *Molecules of Death*, 2nd ed. (London, UK: Imperial College Press, 2007) 149-165.
- [7]. A. Mudhoo, S.K. Sharma, V.K. Garg, and C.-H. Tseng, Arsenic: An Overview of Applications, Health, and Environmental Concerns and Removal Processes, *Critical Reviews in Environmental Science and Technology*, 41, 2011, 435-519.
- [8]. Drinking Water Contaminants, EPA Web Page. <http://water.epa.gov/drink/contaminants/index.cfm> (accessed in July, 2017).
- [9]. D.T. Quang and J.S. Kim, Fluoro- and Chromogenic Chemodosimeters for Heavy Metal Ion Detection in Solution and Biospecimens, *Chemical Reviews*, 110, 2010, 6280-6301.
- [10]. M.R. Knecht and M. Sethi, Bio-Inspired Colorimetric Detection of  $\text{Hg}^{2+}$  and  $\text{Pb}^{2+}$  Heavy Metal Ions Using Au Nanoparticles, *Analytical and Bioanalytical Chemistry*, 394, 2009, 33-46.
- [11]. P.A. Lieberzeit and F.L. Dickert, Sensor Technology and Its Application in Environmental Analysis, *Analytical and Bioanalytical Chemistry*, 387, 2007, 237-247.
- [12]. Q.X. Zhang, D. Peng, and X.-J. Huang, Effect of Morphology of A-MnO<sub>2</sub> Nanocrystals on Electrochemical Detection of Toxic Metal Ions, *Electrochemical Communications*, 34, 2013, 270-273.
- [13]. Z. Lu and Y. Yin, Colloidal Nanoparticle Clusters: Functional Materials by Design, *Chemical Society Reviews*, 41, 2012, 6874-6887.
- [14]. T.K. Sau, A.L. Rogach, F. Jäckel, T.A. Klar, and J. Feldmann, Properties and Applications of Colloidal Nonspherical Noble Metal Nanoparticles, *Advanced Materials*, 22, 2010, 1805-1825.
- [15]. R. Sardar, A.M. Funston, P. Mulvaney, and R.W. Murray, Gold Nanoparticles: Past, Present, and Future, *Langmuir*, 25, 2009, 13840-13851.
- [16]. A.C. Templeton, W.P. Wuelfing, and R.W. Murray, Monolayer-Protected Cluster Molecules, *Accounts of Chemical Research*, 33, 2000, 27-36.
- [17]. M. Brust, M. Walker, D. Bethell, D.J. Schiffrin, and R. Whyman, Synthesis of Thiol-Derivatized Gold Nanoparticles in a Two-Phase Liquid-Liquid System, *Journal of the Chemical Society, Chemical Communications*, 1994, 801-802.
- [18]. J.F. Hicks, D.T. Miles, and R.W. Murray, Quantized Double-Layer Charging of Highly Monodisperse Metal Nanoparticles, *Journal of the American Chemical Society*, 124, 2002, 13322-13328.
- [19]. H. Kuang, W. Chen, W. Yan, L. Xu, Y. Zhu, L. Liu, H. Chu, C. Peng, L. Wang, N.A. Kotov, and C. Xu, Crown Ether Assembly of Gold Nanoparticles: Melamine Sensor, *Biosensors and Bioelectronics*, 26, 2011, 2032-2037.

- [20]. A. Caragheorgheopol and V. Chechik, Mechanistic Aspects of Ligand Exchange in Au Nanoparticles, *Physical Chemistry Chemical Physics*, 10, 2008, 5029-5041.
- [21]. A.J. Bard and L.R. Faulkner, *Electrochemical Methods: Fundamentals and Applications*, 2nd Ed. (New York, NY: John Wiley & Sons, Inc., 2001) Chapter 2.
- [22]. H. Kaiser, Quantitation in Elemental Analysis, *Analytical Chemistry*, 42, 1970, 24A-41A.
- [23]. E. Bakker, Determination of Unbiased Selectivity Coefficients of Neutral Carrier-Based Cation-Selective Electrodes, *Analytical Chemistry*, 69, 1997, 1061-1069.
- [24]. C.J. Pedersen, Crystalline Salt Complexes of Macrocyclic Polyethers, *Journal of the American Chemical Society*, 92, 1970, 386-391.
- [25]. R.D. Shannon, Revised Effective Ionic Radii and Systematic Studies of Interatomic Distances in Halides and Chalcogenides, *Acta Crystallographica A*, 32, 1976, 751-767
- [26]. M. Shamsipur and M.H. Mashhadizadeh, Cadmium Ion-Selective Electrode Based on Tetrathia-12-Crown-4, *Talanta*, 53, 2001, 1065-1071.
- [27]. A.R. Fakhari, M.R. Ganjali, and M. Shamsipur, PVC-Based Hexathia-18-Crown-6-tetraone Sensor for Mercury(II) Ions, *Analytical Chemistry*, 69, 1997, 3693-3696.
- [28]. H.R. Pouretedal and M.H. Keshavarz, Lead(II)-Selective Electrode Based on Dibenzodiazia-15-Crown-4, *Asian Journal of Chemistry*, 16, 2004, 1319-1326.
- [29]. N.W. Alcock, M. Ravindran, and G.R. Willey, Preparations and Structural Correlations for the Complexes of M(III) Halides (M = As, Sb, Bi) with Crown Ethers: Structures of AsCl<sub>3</sub>.12-Crown-4, AsCl<sub>3</sub>.15-Crown-5, SbCl<sub>3</sub>.12-Crown-4 and BiCl<sub>3</sub>.15-Crown-5 and an Evaluation of Relative Binding Strengths for Crown Ligands, *Acta Crystallographica B*, 49, 1993, 507-514.
- [30]. M.A. Munoz-Hernandez, Arsenic: Inorganic Chemistry, in R.B. King (Ed.), *Encyclopedia of Inorganic Chemistry* (New York, NY: John Wiley & Sons, 1994).